Int. J. Multiphase Flow Vol. 19, No. 2, pp. 337–346, 1993
Printed in Great Britain.

0301-9322/93 $6.00 + 0.00

THE EFFECTS OF CONTACT ANGLE ON TWO-PHASE FLOW IN CAPILLARY TUBES

A. M. BARAJAS† and R. L. PANTON
Mechanical Engineering Department, University of Texas at Austin, Austin, TX 78712, U.S.A.

(Received 1 July 1992; in revised form 30 November 1992)

Abstract—A two-phase gas–liquid flow was studied in small diameter (1.6 mm i.d.) horizontal tubes. Adiabatic flow of air–water mixtures was tested over a range of flow rates, 1000:1 for air and 600:1 for water. Flow maps were established for four systems with different contact angles. Each system contained the same fluids (air and water) and had the same tube diameter, however, the tube material was different for each system. The four tube materials were pyrex, polyethylene, polyurethane and FEP, a fluoropolymer resin. Three of the contact angles, measured on a flat sample of each tube material, were partially wetting (34° 61° and 74°) and one was partially non-wetting (106°). The flow maps for the systems were very similar except for a region of rivulet flow. Rivulet flow is a new flow regime that replaces wavy flow when the contact angle becomes large. On the other hand, the transition boundaries for the non-wetting system, except for the plug–slug transition, were significantly changed.

Key Words: two-phase flow, horizontal, capillary, flow patterns

INTRODUCTION

Two-phase flow in tubes occurs in a wide variety of engineering applications. Several examples of two-phase flow in tubes are heat exchangers (including boilers and condensers) and devices for the transfer of cryogenic fluids. The heat transfer, mass transfer and the pressure drop in the tube depend upon how the two fluids are distributed. This distribution of the fluids is called the flow pattern or flow regime. Flow patterns have been reasonably well-defined for modest and large diameter tubes, however for very small diameter tubes research has shown that surface tension forces become important, and the patterns are not as well-defined.

One of the widely used two-phase flow maps was that of Baker (1954). He gathered data from various projects on two-phase flow and prepared a flow map for air–water systems for flow in horizontal tubes ranging from 1″ to 4″. He made an attempt to correct the data for fluid properties, however the correction was not well-verified by experimental data. Taitel & Dukler (1976) developed the first theoretical model which predicted the effects of gas and liquid flow rates, pipe size, fluid properties and angle of inclination upon the transition boundaries. They proposed five dimensionless parameters, based upon the fluid properties and operating conditions, that controlled the transition between flow patterns. They found that the transition from one flow pattern to another was controlled by two or three of these parameters. However, the same set of parameters did not control all of the transition boundaries. Since there was not a common set of parameters which controlled all transitions, it is difficult to develop a single non-dimensional flow map containing all flow patterns. They developed flow maps from their model and found them to be in agreement with the flow maps developed by Mandhane *et al.* (1974). These flow maps were not developed for very small diameter tubes where surface tension becomes an important factor.

Weisman *et al.* (1979) studied the effects of fluid properties and pipe diameter on two-phase flow patterns in horizontal tubes. They studied tube diameters of 11.4, 25.4 and 50.8 mm. These authors concluded that fluid properties had only a small effect upon flow patterns at these tube diameters. Suo & Griffith (1964) performed some of the first studies of two-phase flow in capillaries. They concluded that since capillary slug flow exists in both horizontal and vertical tubes, the surface tension forces dominate over the gravity forces. Damianides & Westwater (1988) studied two-phase flow in tubes ranging from 1 to 5 mm. They concluded that the surface tension between the gas and liquid is a very important variable for two-phase flow in air–water systems with pyrex glass

†Present address: City Public Service, Box 1771, San Antonio, TX 78296, U.S.A.

tube diameters of $\leqslant 5$ mm. Graska (1986), using liquids with different surface tensions, concluded that the liquid–gas surface tension is a significant variable in two-phase flow through pyrex glass tubes with i.d. $\leqslant 5$ mm. Our study is complementary in that we keep the same liquid and gas but change the wall material.

A liquid–gas–solid system is characterized by the surface tension between the gas and liquid and also by the contact angle between the liquid–gas interface and the solid. The idea of the equilibrium contact angle was proposed by Thomas Young over 185 years ago (see Zisman 1964). The equilibrium contact angle is treated as the result of the mechanical equilibrium of a drop of liquid resting on a flat solid surface under the action of three surface tensions (figure 1). Here, σ_{SL} σ_{SG} and σ_{LG} are the surface tensions at the interface between the solid and liquid phases, the solid and gas phases and the liquid and gas phases, respectively. A force balance upon this system yields the following equation:

$$\cos\theta = (\sigma_{SG} - \sigma_{SL})/\sigma_{LG}.$$

In larger diameter tubes, σ_{LG} is of importance because as σ_{LG} increases, liquid droplets form more readily. The concept of the contact angle, θ, is valuable because it provides a definition to the idea of wettability. When $\theta = 0°$, the liquid completely wets the solid surface. A liquid is said to be non-spreading on a certain solid material if $\theta \neq 0°$. When $0° < \theta < 90°$, the liquid partially wets the solid surface. When $90° < \theta < 180°$, the liquid is partially non-wetting; and when $\theta = 180°$, the liquid is completely non-wetting. It should be noted that it is not the intention to use the contact angle (measured on a flat sample of the tube material) as an exact measure of the contact angle in the capillary tube; however, it is intended that θ shows the general surface characteristics of the tube material and the fluids. This study will look at horizontal tubes of very small diameter (1.6 mm i.d.), and use the equilibrium contact angle to classify the results.

EXPERIMENTAL FACILITY

A schematic diagram of the test facility used for the experiments is given in figure 2. Four test sections made of different material, chosen to provide a wide range of contact angles, were used. All test sections consisted of a transparent tube, of 1.6 mm i.d. × 300 mm long, mounted on a ruler. The viewing section was located approx. 160 diameters downstream of the test section entrance. Numerous contact angle measurements were made, both before and after the flow maps were developed, so that a minimal variation in the contact angle could be documented. To provide a mean contact angle, numerous measurements were taken over the entire surface of a flat sample. The four tube materials chosen were pyrex, polyethylene, polyurethane and FEP, a fluoropolymer resin.

The pyrex tube used was a precision bore tube made by Wilmad Glass Co., Buena, NJ. The mean contact angle measured on a flat sample of pyrex obtained from the same company was 34°. All of the plastic tubes, polyethylene, polyurethane and FEP, were provided by Norton Performance Plastics, Elk Grove, IL. The mean contact angle measured on a flat sample of polyethylene was 61°. The mean contact angle for the polyurethane was 74°. It is interesting to note that steel has a contact angle of approx. 70°–90°, when measured with air and water. It is likely that the flow map developed for the polyurethane tube will be very similar to that for water and air in a steel tube. The mean contact angle for the FEP fluoropolymer was 106°. FEP is the only non-wetting material we could find that was also transparent.

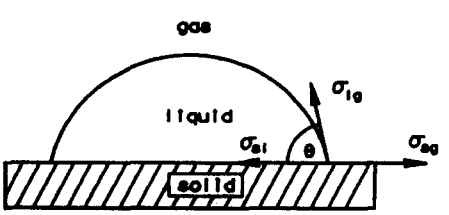

Figure 1. Equilibrium contact angle of a drop of liquid on a solid surface.

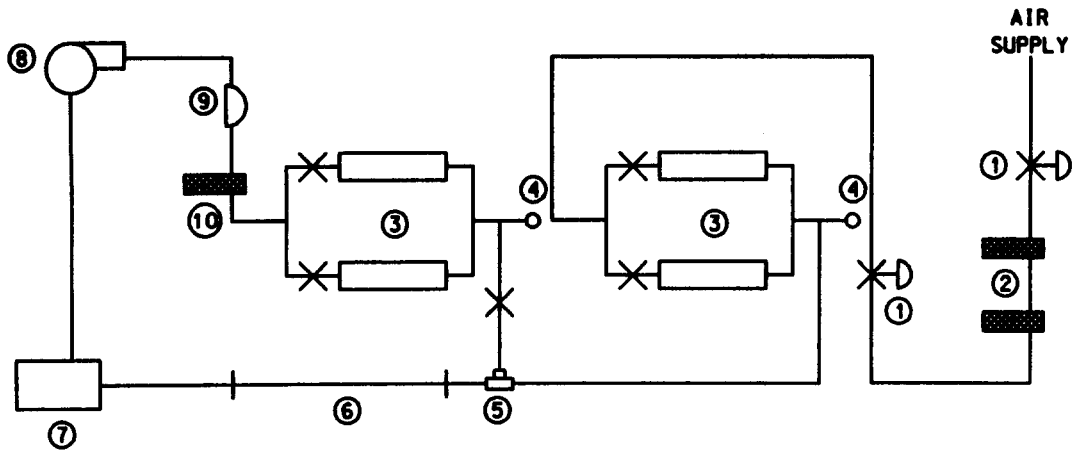

Figure 2. Schematic of the experimental arrangement: 1, gas regulator; 2, gas filter; 3, rotameters; 4, pressure gauge; 5, mixing section; 6, test section; 7, separating reservoir; 8, peristaltic pump; 9, flow integrator; 10, liquid filter.

Flow started from the separating reservoir, which contained untreated tapwater at atmospheric pressure and ambient temperature. The water was pumped using a Masterflex variable-speed peristaltic pump. In a peristaltic pump, the liquid remains in the flexible tubing and does not come in contact with any part of the pump, thus eliminating contamination of the liquid by the pump. Fluctuations in the flow rate generated by the peristaltic pump were damped out using a Cole Palmer flow integrator. A 25.4 cm 30 μm bleached cotton filter was used for water filtration. The large filter helped further damp out any pulsations generated by the pump. The water flow rate was measured using two Omega variable-area rotameters connected in parallel.

Air at approx. 550 kPa from the building's compressed air system was used as the supply. It was then reduced through a regulator to approx. 150 kPa and filtered. The air then passed through another regulator along with the two block valves to control the air flow rate. The air was metered using two Omega variable-area rotameters connected in parallel. The estimated uncertainty in the flow rate measurement is $\pm 5\%$.

Some flow patterns can be determined visually, however in many cases photographs are required. Photographs of the test section were taken using a 35 mm camera with a 2 $\times$ converter and a 50 mm macro lens. The test section was illuminated from the rear by a stroboscope, set to trigger on an external signal.

FLOW PATTERN DEFINITION

In the present study, the occurrence of a specific flow pattern was determined by visual observations, aided by a stroboscope and by photographic techniques. Some differences exist among the various researchers' definitions of two-phase flow patterns. Since flow pattern identification by visual observation is subjective, it is essential to define the flow patterns in detail. The flow patterns described below are a combination of, and are consistent with, the flow patterns described by Colin *et al.* (1991), Graska (1986) and Wambsganss *et al.* (1991), modified for tube flow. The only exceptions being the "rivulet" and "multiple rivulet" flow patterns which are terms to describe two new flow patterns encountered in this study. Figure 3 illustrates the flow patterns considered in this study.

(a) **Wavy.** A stratified flow with waves at the interface that travel in the direction of the flow. The waves do not reach the top of the tube.
(b) **Plug.** This flow pattern contains intermittent *plugs of gas* (elongated bubbles longer than one tube diameter) surrounded by a continuous liquid phase. The radial diameters of the plugs tend to increase with increasing gas flow rates.
(c) **Slug.** This flow pattern contains intermittent *slugs of liquid* formed by waves of liquid growing until they touch the top of the tube. The slug, which travels at

approximately the same rate as the gas, blocks the entire cross section of the tube and keeps its identity until it reaches the exit of the tube.

(d) **Annular.** In this flow pattern the liquid flows in a film along the tube wall and the gas flows through the center. Roll waves generally propagate down the tube length at the liquid–gas interface.

(e) **Bubble.** This flow pattern contains dispersed vapor distributed as discrete small bubbles in the continuous liquid phase. The number of bubbles increases with increasing gas flow rate until the entire tube cross section becomes filled with bubbles.

(f) **Dispersed.** This flow pattern is very similar to the annular flow pattern, except the majority of the liquid is entrained as droplets in the gas flow. The liquid film on the tube surface still exists.

(g) **Rivulet.** A stream of liquid flows on the tube surface. The stream generally does not flow straight down the tube length, but twists its way down the tube length much like a river. The stream of liquid may be found flowing on the bottom or sides of the tube, as well as the top of the tube.

(h) **Multiple rivulet.** This flow pattern is very similar to the rivulet flow pattern, except that multiple streams of liquid propagate down the tube length of the tube surface.

It should be noted that all of these flow patterns do not exist on any one particular flow map. For instance, the rivulet and multiple rivulet flow patterns do not appear on the map for the pyrex tube ($\theta = 34°$), while the wavy flow patterns exists only on this flow map.

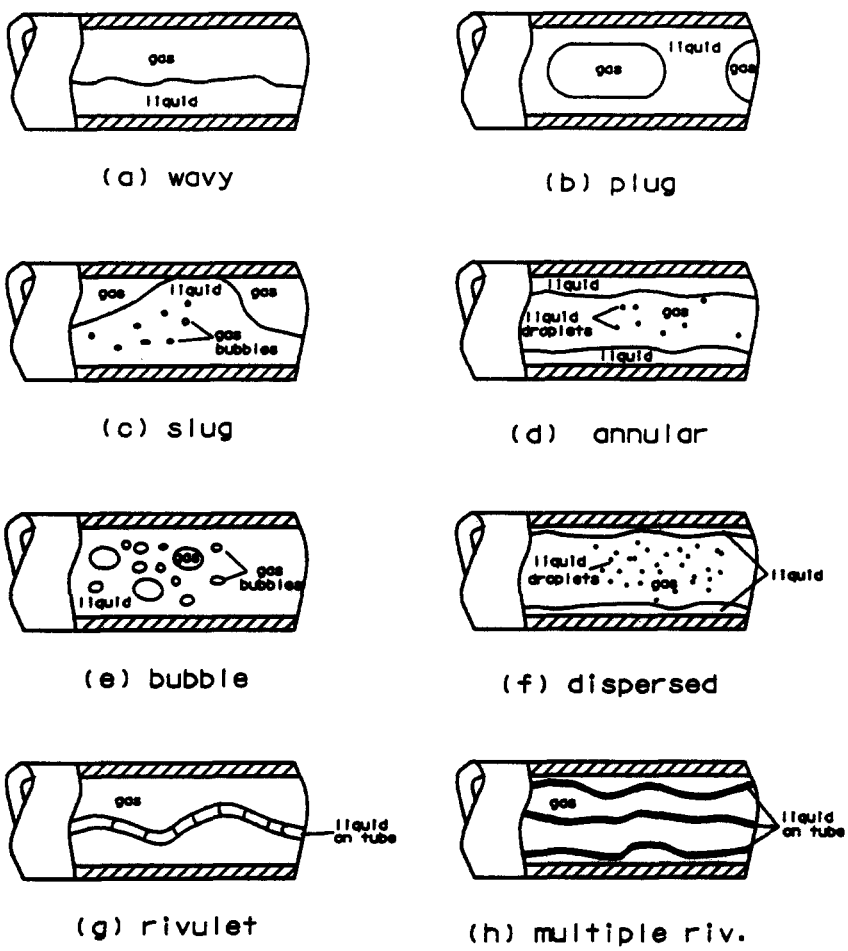

Figure 3. Flow patterns defined for this study.

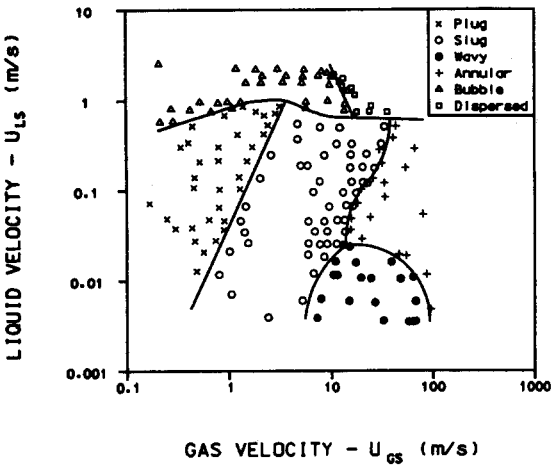

Figure 4. Flow map for the pyrex–water–air system ($\theta = 34°$).

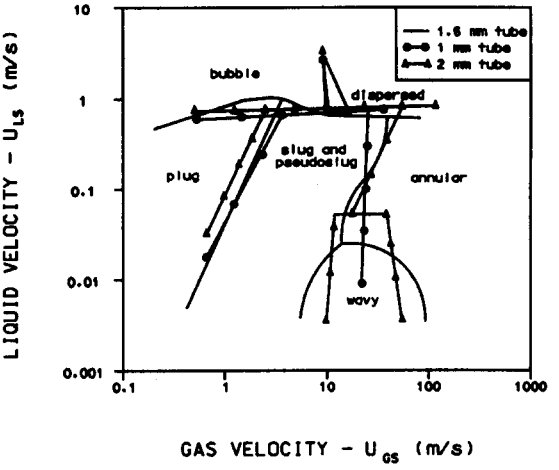

Figure 5. Comparison of the pyrex flow map, 1.6 mm, with maps of Damianides & Westwater (1988) for 1 and 2 mm tubes.

EXPERIMENTAL PROCEDURE

For each of the systems studied, the superficial gas velocity (the velocity that would occur if the same flow rate of gas occupied the entire tube) was varied from approx. 0.1 to 100 m/s, while the superficial liquid velocity was varied from approx. 0.003 to 2 m/s. In the sequence of testing the superficial velocities were varied from left to right and from bottom to top on the flow map. That is, increasing the gas velocity while maintaining a constant liquid velocity. The liquid velocity was then increased and the procedure was repeated until the full range of velocities was covered. In areas of the flow map where the transition zone was almost horizontal, the liquid velocity was increased while the gas velocity was held constant. The maps were developed in the above fashion because there appeared to be a slight hysteresis in the transition boundary in all of the systems studied, with the exception of the pyrex system ($\theta = 34°$). For instance, the transition boundary between slug and annular flow would shift slightly toward lower gas velocities if it were approached from higher gas velocities. This hysteresis was relatively small and no attempt was made to quantify its magnitude.

Water is notorious for picking up contaminates. A procedure was adopted to keep the contamination of the water and test section to a minimum. The test section was cleaned each morning before gathering data by drawing alcohol through the test section in a manner similar to that described by Schwartz *et al.* (1964). Fresh water was placed in the system prior to developing each flow map. Although the water was recirculated, and thus a closed system, it was exposed to the atmosphere while in the separating reservoir. As mentioned previously, there was no contamination from the pump due to the nature of the peristaltic pump. In order to document that contamination was being controlled, numerous contact angle measurements were made both before and after developing each flow map. It was evident from these measurements that contamination of the water had only a negligible effect upon the contact angle.

RESULTS

The flow map developed for the pyrex tube ($\theta = 34°$), with a nominal inside diameter of 1.5875 mm ($\frac{1}{16}''$) is shown in figure 4. The pyrex flow map may be thought of as a base map because there have been a number of studies done on two-phase flow through pyrex tubes. One can see in figure 4 that numerous data points were required in order to define the transition lines. Figure 5 shows the present flow map along with maps developed by Damianides & Westwater (1988) for 1 and 2 mm pyrex tubes, so these two diameters bracket our 1.6 mm tube. These authors found a strong effect of diameter (surface tension). The pyrex tube used in the present experiment was obtained from the same company as the 1 and 2 mm tubes cited above. There are several features

of these maps that need to be noted. Foremost is that Damianides & Westwater's (1988) map for the 2 mm tube contains a region where wavy flow exists but the 1 mm map does not. Also, their flow maps contain a flow pattern (not shown) in the upper right portion of the slug region entitled "pseudoslug". Visually, this flow pattern looks very similar to slug flow, however, the pressure fluctuations are different from that of slug flow. This topic is discussed by Lin & Hanratty (1987). Since the present study did not have fast response pressure instrumentation, this pseudoslug flow could not be identified. Finally, there is a slight difference in the definition of the bubble flow pattern between the two studies. Considering these differences, the present flow map, which has a wavy flow region, is in good agreement with the 2 mm map of Damianides & Westwater (1988).

Figure 6 shows the flow map for the polyethylene tube ($\theta = 61°$). This map is similar to the flow map for the pyrex tube ($\theta = 34°$), except the wavy flow pattern was not observed. Instead, a rivulet flow pattern occupies the region on the flow map where the wavy flow pattern existed on the pyrex map. Since the polyethylene system is less wetting than the pyrex system (the tension σ_{SL} has decreased), the contact line of the water can be displaced more readily. The flow map developed for the polyurethane tube ($\theta = 74°$) is shown in figure 7. This flow map appears very similar to the flow map for the polyethylene tube ($\theta = 61°$), however, another alteration has occurred. At high gas velocities there is a small region of the multiple rivulet flow pattern. Since the polyurethane system has an even lower σ_{SL}, higher θ, at high gas velocities the shear forces cause the single rivulet to break into several streams.

All of the previous data are for partially wetting systems. The only partially non-wetting system is shown in figure 8 for the FEP fluoropolymer tube ($\theta = 106°$). This flow map is quite different from the maps developed for the partially wetting systems. There is a considerable increase in the size of the multiple rivulet flow region at the expense of a reduced annular flow region. Because the fluid is partially non-wetting, σ_{SL} has now decreased to be smaller than σ_{SG}. The other characteristics for the $\theta = 106°$ system are best seen in figure 9.

Figure 9 shows all four flow maps on the same plot. The first obvious effect of the contact angle is the two new rivulet flow patterns. The second effect is in the partially wetting systems where the contact angle is $<90°$. For these systems the contact angle has little effect upon the transition boundaries between plug and bubble flow, slug and bubble flow, slug and dispersed flow or slug and annular flow. For all systems, regardless of the wettability, the contact angle has a minimal effect upon the transition boundaries between plug and slug flow and between bubble and dispersed flow.

The biggest change in the transition boundaries occurs for the partially non-wetting FEP fluoropolymer tube ($\theta = 106°$). For this system, the transition boundaries between slug and rivulet flow and between slug and annular flow are moved to the left to lower gas velocities. Since this system ($\theta = 106°$) is partially non-wetting, the liquid is moved by shear forces much easier than in the partially wetting systems ($\theta = 34°$, 61° and 74°), thus requiring a lower gas velocity for the

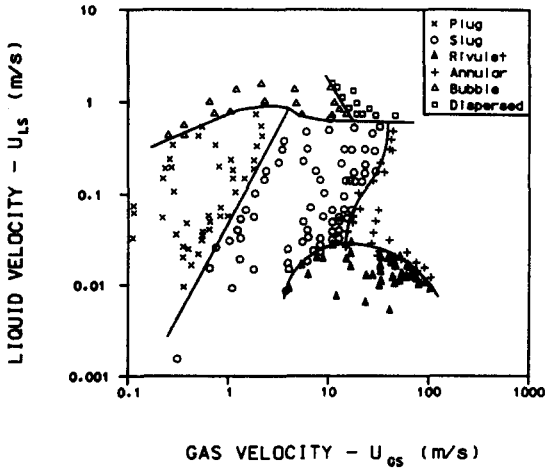

Figure 6. Flow map for the polyethylene tube ($\theta = 61°$).

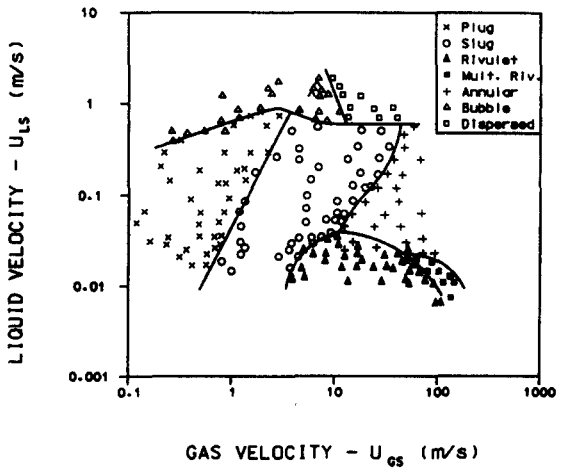

Figure 7. Flow map for the polyurethane tube ($\theta = 74°$).

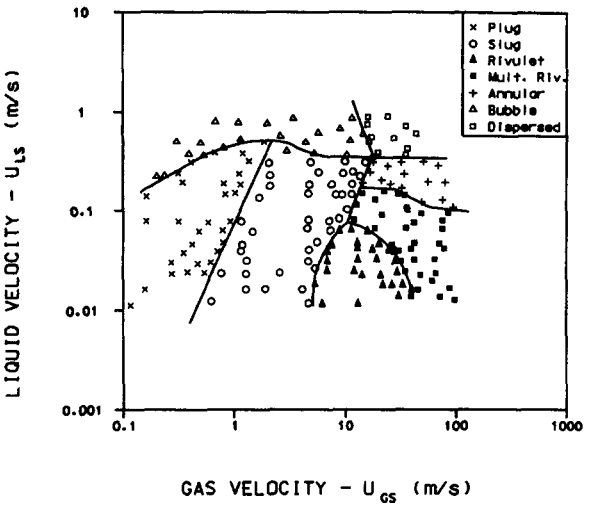

Figure 8. Flow map for the FEP fluoropolymer tube ($\theta = 106°$).

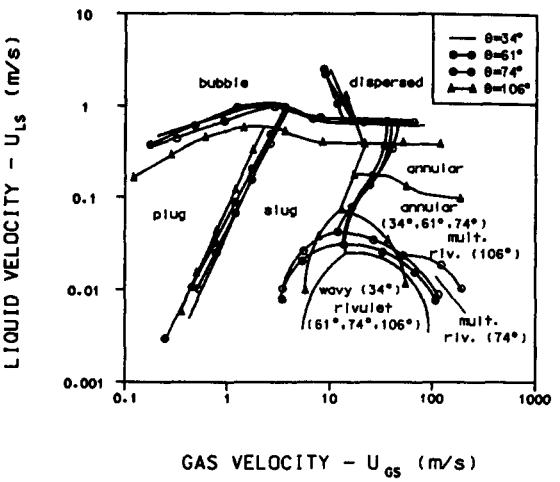

Figure 9. Comparison of contact angle effects.

transition to multiple rivulet or annular flow. Another change is that the transition boundaries between plug and bubble flow, slug and bubble flow and annular and dispered flow are at lower liquid velocities.

For $\theta = 34°$, rivulet flow is not observed. The rivulet flow pattern is very sensitive to the contact angle, and with increasing contact angle it exists at higher liquid velocities. This is because the increased contact angle inhibits the liquid from spreading on the tube wall, thus preventing the annular flow from developing. When the fluid is non-wetting, the transition from multiple rivulet

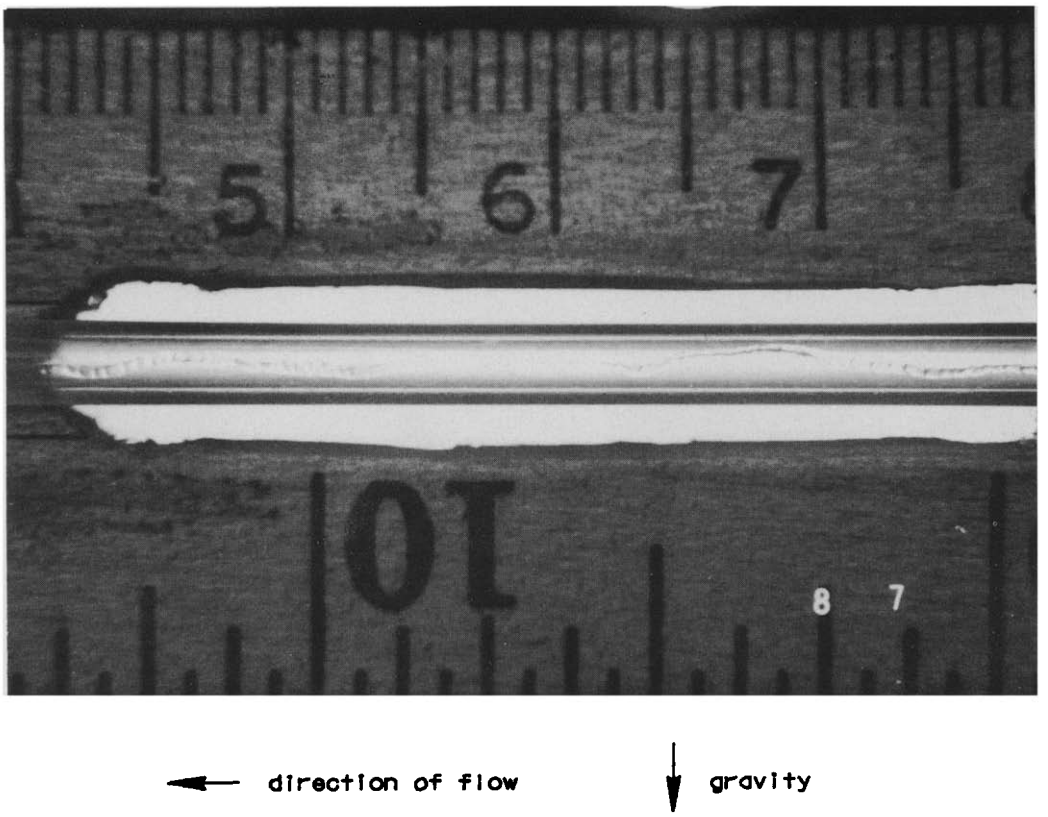

Figure 10. Rivulet flow in the FEP fluoropolymer tube ($\theta = 106°$); $U_{GS} = 24.7$ m/s, $U_{LS} = 9 \times 10^{-3}$ m/s.

to annular flow occurs at relatively high liquid velocities. This high contact angle prevents the liquid from spreading on the tube, thus allowing more liquid to be carried by a rivulet.

Still photographs were taken to aid visual observations, and to document the rivulet flow patterns observed in this study. Each photograph contains two scales, the smaller scale having metric units with the minor division equal to 1 mm, and the larger scale having imperial units with the major division equal to 1″. In all photographs the flow is from right to left and gravity is directed downward. Figure 10 shows rivulet flow in the FEP fluoropolymer tube ($\theta = 106°$). The superficial liquid velocity was 0.009 m/s, while the superficial gas velocity was 24.7 m/s. In this photograph the tube wall is not wetted, except where the stream of water is flowing on the side of the tube. Figure 11 shows multiple rivulet flow in the FEP fluoropolymer tube. The superficial liquid velocity was 0.014 m/s and the superficial gas velocity was 75.8 m/s. This photograph shows three visible streams of water flowing on the front side of the tube. One stream is approximately midway between the bottom and the center of the tube, one stream is flowing approximately midway up the tube surface and one stream is flowing on the top of the tube. Figure 12 shows bubble flow in the pyrex tube ($\theta = 34°$). The superficial liquid velocity was 0.946 m/s, while the superficial gas velocity was 0.45 m/s. Note that the bubbles are smaller than one tube diameter. In this photograph it can be seen that body forces do not dominate, because the bubble density is not greater along the top of the tube.

CONCLUSIONS

The prior work of Damianides & Westwater (1988) and Graska (1986) showed that the surface tension between the liquid and gas is an important parameter in the flow through capillary tubes. It is evident from the data obtained in this study that the contact angle is also a significant variable for two-phase flow in capillary tubes.

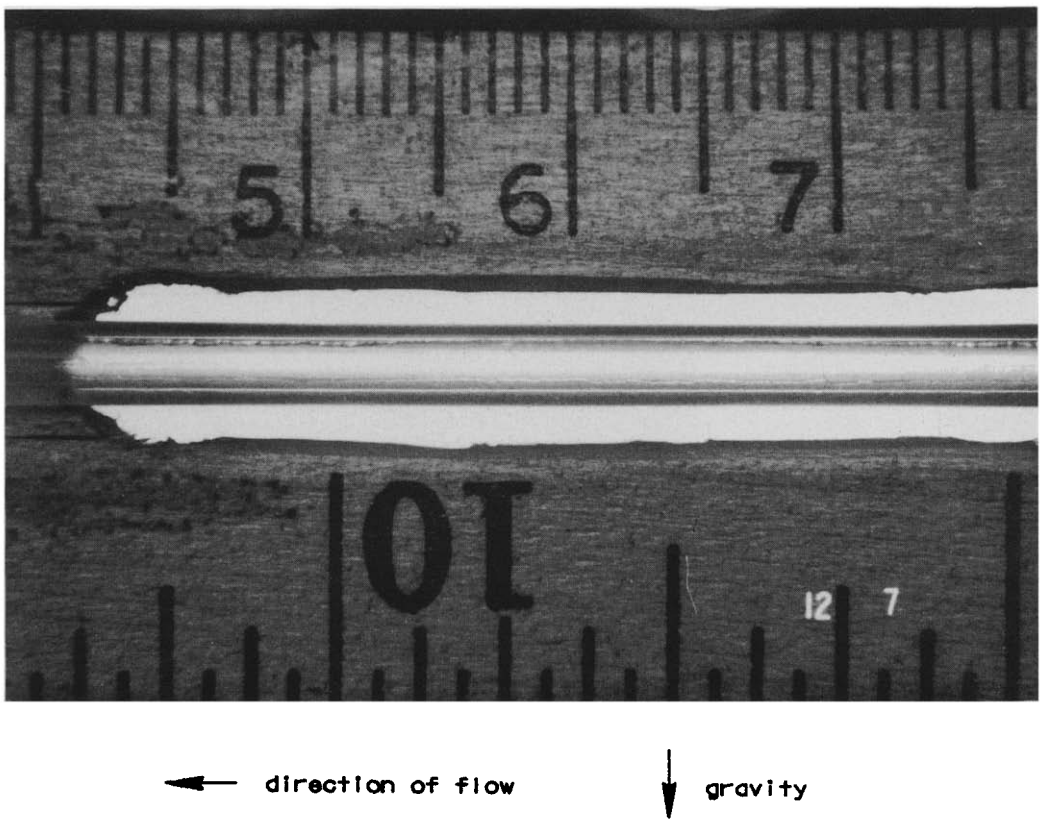

Figure 11. Multiple rivulet flow in the FEP fluoropolymer tube ($\theta = 106°$); $U_{GS} = 75.8$ m/s, $U_{LS} = 0.014$ m/s.

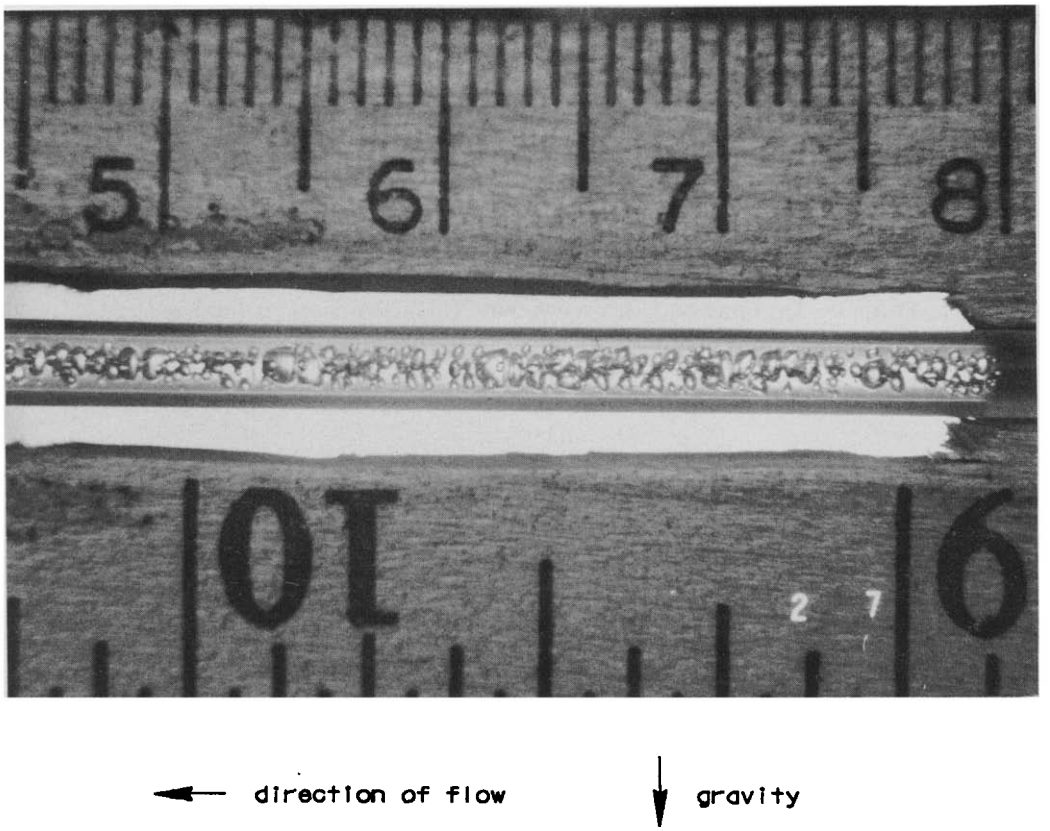

Figure 12. Bubble flow in the pyrex tube ($\theta = 34°$); $U_{GS} = 0.45$ m/s, $U_{LS} = 0.946$ m/s.

It was found that in the partially wetting systems ($\theta < 90°$), the contact angle had little effect upon the transition boundaries, with one exception. Between $\theta = 34°$ and 61° the wavy flow regime becomes a rivulet flow. Gravity no longer confines the flow to the bottom of the tube. With higher contact angles, $\theta = 74°$, and high gas velocities the rivulet breaks up into several rivulets.

In the partially non-wetting system ($\theta > 90°$), the contact angle had a significant effect upon certain transition boundaries. Those boundaries that moved significantly were between plug and bubble flow, between slug and bubble flow, between annular and dispersed flow, between slug and multiple rivulet flow and between slug and annular flow.

It was found that varying the contact angle had little effect upon the transition boundary between certain flow patterns. The transition boundaries not affected by the contact angle were between plug and slug flow and between bubble and dispersed flow.

REFERENCES

BAKER, O. 1954 Simultaneous flow of oil and gas. *Oil Gas J.* **53,** 185–195.

COLIN, C., FABRE, J. & DUKLER, A. E. 1991 Gas–liquid flow at microgravity conditions—I. Dispersed bubble and slug flow. *Int. J. Multiphase Flow* **17,** 533–544.

DAMIANIDES, C. A. & WESTWATER, J. W. 1988 Two-phase flow patterns in a compact heat exchanger and in small tubes. In *Proc. 2nd UK Natn Conf. on Heat Transfer*, Vol. II, pp. 1257–1268.

GRASKA, M. L. 1986 Effects of fluid surface tension and tube diameter on horizontal two-phase flow in small diameter tubes. M.S. Thesis, Univ. of Illinois at Urbana-Champaign, IL.

LIN, P. Y. & HANRATTY, T. J. 1987 Detection of slug flow from pressure measurements. *Int. J. Multiphase Flow* **13,** 13–21.

MANDHANE, J. M., GREGORY, G. A. & AZIZ, K. 1974 A flow map for gas–liquid flow in horizontal pipes. *Int. J. Multiphase Flow* **1,** 537–553.

SCHWARTZ, A. M., RADER, C. A. & HUEY, E. 1964 Resistance to flow in capillary systems of positive contact angle. In *Contact Angle Wettability and Adhesion*, pp. 250–267. American Chemical Society, New York.

SUO, M. & GRIFFITH, P. 1964 Two-phase flow in capillary tubes. *Trans. ASME Jl Bas. Engng* **86,** 576–582.

TAITEL, Y. & DUKLER, A. E. 1976 A model for predicting flow regime transition in horizontal and near horizontal gas–liquid flow. *AIChE Jl* **22,** 47–55.

WAMBSGANSS, M. W., JENDRZEJCZYK, J. A. & FRANCE, D. M. 1991 Two-phase flow patterns and transitions in a small, horizontal, rectangular channel. *Int. J. Multiphase Flow* **17,** 47–55.

WEISMAN, J., DUNCAN, D., GIBSON, J. & CRAWFORD, T. 1979 Effects of fluid properties and pipe diameter on two-phase flow patterns in horizontal lines. *Int. J. Multiphase Flow* **5,** 437–462.

ZISMAN, W. A. 1964 Relation of equilibrium contact angle to liquid and solid constitution. In *Contact Angle Wettability and Adhesion*, pp. 1–51. American Chemical Society, New York.